Nuclear medium effects in muonic neutrino interaction with energies from 0.2 GeV to 1.5 GeV

D. Vargas, A.R. Samana,* F.G. Velasco, O.R. Hoyos, and F. Guzmán

Universidade Estadual de Santa Cruz - UESC, Rodovia Jorge Amado km 16, Ilhéus, 45662-900, Brasil

J.L. Bernal-Castillo, E. Andrade-II, R. Perez, and A. Deppman

Instituto de Física da Universidade de São Paulo-IFUSP, Rua do Matão, Travessa R, 187, São Paulo, 05508-090, Brasil

C.A. Barbero and A.E. Mariano

Instituto de Física La Plata-CONICET, 49 y 115, La Plata, CP 1900, Argentina.

(Dated: September 19, 2018)

Nuclear reactions induced by muon neutrino with energies in the range from 0.2 to 1.5 GeV in Monte Carlo calculations framework in the intra-nuclear cascade model are studied. This study was done by comparison between the available experimental data and theoretical values of total cross section, and the energy distribution of emitted lepton energy in the reaction muon neutrino-nucleus, using the targets: ^{12}C, ^{16}O, ^{27}Al, ^{40}Ar, ^{56}Fe and ^{208}Pb. A phenomenological toy model of primary neutrino-nucleon interaction gives a good agreement of our theoretical inclusive neutrino nucleus cross in comparison with the available experimental data. Some interesting results on the behavior of the cross section as function of 1p-1n and higher contributions are also sketched. The previous results on the percentage of fake events related in available experiments in ^{12}C were expanded for the set studied nuclei. With the increase of mass target, the nuclear effects in the cross sections were observed along with the importance to take into account fake events in the reactions.

PACS numbers: 13.15.+g, 25.30.Pt, 24.10.Lx

I. INTRODUCTION

The investigation of neutrino-nucleus interaction is a field that gained an increasing relevance in recent years allowing studies on neutrino oscillation and the neutrino massiveness [1]. Moreover, neutrino-nucleus interaction plays a key role in Astrophysics issues such as supernova dynamics [2].

From the experimental side, a special difficulty faced in the study of neutrino interactions is the fact that the neutrino energy is unknown, being described by broad energy distributions. This problem prevents the extraction of information concerning to essential characteristics of neutrinos [1], which requires their reconstruction fluxes from final states measurements. Furthermore, final states are strongly dependent on nuclear properties and nuclear effects.

Within the treatment of weak interaction in the nuclear medium appear complex processes due to the effects of nuclear structure and interactions between the various nucleons. There are several theoretical models in the description of neutrino-nucleus/nucleon cross sections. A few of them have been implemented in computer numerical codes to simulate the interactions in several neutrino experiments in progress. Many of the used formalisms do not have a specific name, and here we will distinguish them with the name of the numerical code such as GENIE [3], NUANCE [4], between others. Further, there is another, not yet implemented theoretical formalism called Consistent Isobar Model-CIM [5, 6].

Many of these codes are using Monte Carlo (MC) procedures to simulate the reactions in the nuclear cascade. Some important notes are claimed by Ref. [1]: (i) presently available generators all rely on free-particle MC cascade simulations that are applicable at very high energies with limited applicability in the description of relatively low energy with Final States Interactions (FSI) inside the target nuclei; (ii) it is neglected the binding in nuclei and; (iii) some generators are working with outdated nuclear physics and there is not an internal consistency between the different reaction channels.

Another important task that the simulation program and event generator should take into account is the elimination of those so-called fake events, from secondary interactions that introduce noise in the main channel. These secondary interactions are into a more fundamental level of neutrino-nucleon interaction theory, requiring a deep understanding of this interaction. In many neutrino experiments are emitted neutrinos by secondary decays of pions and kaons, usually produced in high energy proton-nucleon/nucleus collisions. For example, in the K2K (Kamioka to Kamioka) [7, 8] experiment a proton beam of 12.9 GeV collides against Al. In the MiniBooNE experiment (Mini Booster Neutrino Experiment) [10, 11], a proton beam of 8.9 GeV collides against Be, forming the so-called long-range beam Long Base Line (LBL). The beams produced in LBL range, from hundreds of MeV to several GeV, are detected hundreds of kilometers away. In this energy range, the dominant contribution to the neutrino-nucleus cross section comes from reactions with charged current (CC) in the channels: quasi-elastic (CCqe) and resonance (CCres) production. There are currently several LBL type experiments in progress, designed to determine the differences between the masses of different kinds of neutrinos and oscillation parameters. In this work we do not analyze the effect on neutral current on the target nuclei here studied, due that the CCqe scattering is the dominant neutrino interaction process for ν_μ

* arsamana@uesc.br

and $\bar{\nu}_\mu$ colliding with a nuclear target when the neutrino energies are on the order 1 GeV [13], On the other hand, Ericson *et. al* [14] have called the attention in the sense that ν_μ neutral current could be necessary to solve the MiniBooNE low-energy anomaly.

The CCqe process

$$\begin{aligned} \nu_l + n &\to l^- + p, \\ \bar{\nu}_l + p &\to l^+ + n, \end{aligned} \tag{1}$$

represents the simplest form of neutrino-nucleon (antineutrino-nucleon) interaction, where the weak charged current induces a transition of neutrino (antineutrino) into its corresponding lepton charged l^- (l^+), that results in the signal of an event. The FSI may lead to more than one ejected nucleon , plus a lepton , and resonances produced by absorp tion of emitted pions can also lead to more ejected nucleons. These last two contributions affect the reconstruction of energy and production of quasi-elastic fake events. Many experiments try to reduce these uncertainties using a near detector and implementing some correlation with the far main detector. Nevertheless, there are no previous studies on how the event generator manages these fake events other than the works of Lalakulich and Mosel [15, 16] and alternatively, Ericson *et. al* [14] in the quasi-elastic reaction of $\nu_\mu{-}^{12}$C.

In the present paper, we show recent developments on the inclusion of neutrino-nuclear interaction in the CRISP (**C**ollaboration **R**io-**I**lhéus-**S**ão **P**aulo) model [17]. CRISP is a nuclear reaction model based on Quantum Dynamics (QD) and Monte Carlo (MC) methods and has being developed for the last two decades [17–21, 23]. CRISP provides reliable descriptions of many-body interactions for photons and electrons, for protons and neutrons, and has being applied to study reactions in nuclei from ^{12}C to ^{240}Am. The incident particles can have energies from 50 MeV up to tens of GeV, and many aspects of nuclear reaction can be investigated, such as specific cross sections, particle multiplicity, and particle spectra, between others. Additionally, the CRISP model has been employed for the investigation of electron scattering [24], meson production in nuclei [21], ultra-peripheral collisions at LHC energies [23], and Λ non-mesonic decay in the nuclear medium [25, 26] using the smallest numbers of possible free parameters. CRISP has not been used before to study neutrino-nucleus interaction, then this work is the first study to this issue.

Further, it is a useful tool to study nuclear effects on different nuclear reactions, which is not the usual case for codes built as event generators, where many parameters must be adjusted for specific reactions. In this paper, we focus on the nuclear effects in neutrino-nucleus reaction. For this purpose, we first include a simple toy model of the primary neutrino-nucleon interaction in the CRISP code, and then analyze how the nuclear effect modifies the different observables.

The paper is organized as follows: in section II we describe briefly the CRISP model and introduce a simple toy model for the neutrino-nucleon interaction that was coupled to CRISP code. In section III, the results are presented and discussed. Finally, in section IV we show our conclusions and final remarks.

II. THEORETICAL MODEL

The study of nuclear reactions must consider all relevant effects due to the nuclear medium. In this paper, we used the CRISP model for the calculation of nuclear reactions. The CRISP code was developed to describe the most relevant nuclear processes realistically. In the following, are presented the most important aspects regarding the nuclear medium.

A. CRISP

QD method and MC method [17] are used in the CRISP model to describe the nuclear processes that take place during a nuclear reaction. In CRISP code, the target is constructed as a Fermi gas where the Fermi energies for protons and neutrons, respectively, are

$$\begin{aligned} E_F^{(p)} &= \frac{1}{2\,m_0}\,(3\pi^2)^{2/3}\left(\frac{Z}{L^3}\right)^{2/3}, \\ E_F^{(n)} &= \frac{1}{2\,m_0}\,(3\pi^2)^{2/3}\left(\frac{A-Z}{L^3}\right)^{2/3}. \end{aligned} \tag{2}$$

where, $L^3 = \frac{4}{3}\,\pi r_0{}^3\,A$, is the nuclear volume, with $r_0 = 1.18$ fm, and m_0 is the rest nucleon mass. The ground state from the momentum space is always generated, including the degrees of freedom related to spin. The respective Fermi momenta for protons and neutrons are given by

$$\begin{aligned} k_F^{(p)} &= \sqrt{E_F^{(p)}(E_F^{(p)} + 2m_0)}, \\ k_F^{(n)} &= \sqrt{E_F^{(n)}(E_F^{(n)} + 2m_0)}. \end{aligned} \tag{3}$$

The momentum space is divided into cells of width Δp calculated as

$$\Delta p = \frac{k_F}{N_l}, \tag{4}$$

where N_l represents the number of levels in the Fermi gas. All nucleons are evenly distributed inside the nuclear volume.

The nuclear reaction in the CRISP model is considered as a two-step calculation process. The first one is the intranuclear cascade, described by the Monte Carlo MultiCollisional (MCMC) model [27]. The second step is the evaporation-fission competition, described by Monte Carlo Evaporation-Fission (MCEF) model [28, 29]. The emphasis of this work is on the intranuclear cascade step since the particles of interest (muon, muon neutrinos, and pions) are emitted only during this step. For the sake of completeness, it must be mentioned that in the evaporation-fission part the Weisskopf's model is used to describe the nuclear de-excitation process by successive evaporation of nucleons or by nuclear fission [20, 29–31]. In the case of fission, the fragments are generated following the Random Neck Rupture Model (RNRM) [32] with symmetric, asymmetric and super-asymmetric channels [33, 34] for the fragments formation. Besides, we include the evaporation of hot fission fragments.

In the intranuclear cascade step, binary interactions only can occur. The multicollisional approach implies that all nucleons move simultaneously [27]. Such an approach makes it natural to check dynamical aspects such as changes in the nuclear density and the evolution of the occupancy levels of the Fermi gas [17, 35]. The Fermi motion of nucleons, also a result of this approach, modifies the nuclear cross sections, especially near the threshold of the interaction. The ordered sequence of collisions considers the probability of interaction with all particles, based on their respective cross sections.

The intranuclear cascade starts with the primary collision when the incident particle interacts on the surface a nucleon of the system or more internally in the nucleus. As a result, secondary particles are produced which have relatively high energy compared to the energy of the others nucleons in the nuclear medium. These particles are called cascade particles. The secondary particles propagate inside the nucleus and can interact with other particles, or they can be emitted when reach the nuclear surface just as their kinetic energy is higher than the nuclear potential or, be reflected continuing their propagation in the nucleus. The nuclear potential is a square well such that

$$V_0 = E_F + B, \tag{5}$$

where B is the binding energy, ~ 8 MeV. The CRISP model also considers the effect of tunneling of charged particles through the Coulomb barrier.

The cascade is completed when there is no resonance yet to decay or hadrons with kinetic energy greater than the nuclear potential. After this condition is satisfied, the remaining excitation energy is evenly distributed between the nucleons in a process known as thermalization. The main characteristics of the nucleus does not change at this stage, so that its atomic number, mass number, and excitation energy remain the same ones until the end of the process [17, 35].

Another fundamental characteristic of CRISP is the strict verification of the Pauli exclusion principle [17], possible thanks, both to the application of the Fermi gas model and the multicollisional approach which to be known enables the 4-vectors of all nucleons at each step of intranuclear cascade.

B. Implementation of the muon neutrino channel as an event generator of the intranuclear cascade

1. *Primary interaction*

The energy range of the muonic neutrino in this paper is $0,2$ - $1,5$ GeV. The most important channels in this energy range are the quasi-elastic scattering and the resonance production. The formation of the Δ (1232) dominates the resonance production, which subsequently decays into a pion and a nucleon. The first step to study the nuclear effects in neutrino-nucleus interaction is to incorporate the primary neutrino-nucleon interaction in the CRISP model. In this way we are considering the neutrino-nucleus interaction as an incoherent sum of the contributions from all nucleons inside the nucleus. Besides, CRISP calculates many nuclear effects as those due to the Fermi motion and to the antisymmetrization of the nuclear wave-functions, as described in subsection II A, as well as all the possible particle-hole states formed due to final state interactions (labeled as npnh events). In the present work, we will not be considered a possible coherent contributions.

Here, the primary neutrino-nucleon interaction is formulated through a toy model where are exactly considered kinematic and isospin aspects of the interaction.

Due to the limitations of the CRISP model, where the nuclear states are described as a Fermi gas, the angular momentum is not a conserved quantity. For these reasons, all our calculations are averaged on the spin states, and an important consequence is the fact that we will not be able to describe angular distributions correctly. In the following, the model for the primary interaction is referred as Kinematic Model (KM).

In our model, the neutrino is supposed to interact with a single nucleon, and since our goal is to analyze the interaction near the threshold region, we consider two interaction channels, namely, the quasi-elastic and the $\Delta-$resonance formation, described below.

2. *Quasi-elastic channel*

The CCqe channel corresponds to a quasi-elastic interaction between neutrino and nucleon where the charged current induces isospin modification of the nucleon. In the process, the neutrino is absorbed and a muon is produced. This process is indicated in Table I.

The empirical formula that gives the CCqe cross section per nucleon is

$$\sigma^{(CCqe)} = \sum_{n=0}^{4} A_n E_\nu^n. \tag{6}$$

We implemented in the code the Equation (6), being the best fit polynomial of order 4th for experimental deuteron experimental data in the range of interest. The coefficients A_n are shown in Table I.

3. *Resonant channel*

In the initial state, we have a nucleon N with momentum p_N a nd a neutrino ν with momentum p_ν. This state is represented by $|N,\nu\rangle_{s,\tau}$, where s,τ are the total spin and isospin of the system neutrino-nucleon. Let be $g_{s,\tau}^{s',\tau'}$ the coupling constant for the neutrino-nucleon vertex, and s',τ' the spin and isospin of the final state.

We are interested in resonant states, so we project the final states onto the resonant states, resulting in

$$|\Psi_\Delta\rangle = A\int d^4p_\Delta \int d^4p_l \sum_{ss'} |\Delta,l\rangle \times \langle\Delta,l|_{s',\tau'}\, g_{s,\tau}^{s',\tau'}\, |N,\nu\rangle_{s,\tau} \times \delta^4(p_\Delta - p_l - p_N - p_\nu), \tag{7}$$

with A being a normalization constant, p_Δ and p_l are, respectively the resonance and lepton momentum. We sum over all

TABLE I. Correspondence between the different labels and relevant parameters for each primary interaction used in this work. The A_n coefficients are in units of 10^{-38} cm^2. The coefficients σ_0 are dimensionless.

Process	Channel	Parameters	Label
CCqe	$\nu_\mu + n \to \mu^- + p$	$A_0 = (2.77 \pm 1.30) \times 10^{-2}$ $A_1 = (1.07 \pm 0.48)$ $A_2 = (-1.01 \pm 0.31) \times 10^{-1}$ $A_3 = (-2.45 \pm 0.25) \times 10^{-1}$ $A_4 = (7.32 \pm 1.30) \times 10^{-2}$	A
		σ_0	
CCres	$\nu_\mu + p \to \mu^- + \Delta^{++} \to \mu^- + \pi^+ + p$	0.66 ± 0.12	B
	$\nu_\mu + n \to \mu^- + \Delta^{+} \to \mu^- + \pi^+ + n$	$0,26 \pm 0,07$	C
	$\nu_\mu + n \to \mu^- + \Delta^{+} \to \mu^- + \pi^0 + p$	$0,25 \pm 0,07$	D

possible spin configuration and

$$
\begin{aligned}
|\Delta, l\rangle_{\tau'} &= \sum_{s'} |\Delta, l\rangle_{s',\tau'} , \\
|N, \nu\rangle_{\tau} &= \sum_{s} |N, \nu\rangle_{s,\tau} ,
\end{aligned} \tag{8}
$$

then

$$
|\Psi_\Delta\rangle = A \int \frac{1}{E_l} d^3p_l \int dm_\Delta |\Delta, l\rangle_{\tau' \tau'} \langle \Delta, l| g_\tau^{\tau'} |N, \nu\rangle_\tau , \tag{9}
$$

where was performed the integration on d^3p_Δ, then $p_\Delta = p_N + p_\nu + p_l$, and the coupling constant for the neutrino-nucleon vertex was renamed for simplicity of notation, $g_{s,\tau}^{s',\tau'} \equiv g_\tau^{\tau'}$. This integration on m_Δ is equivalent to the integration of the total Δ energy, E_Δ.

The resonant state propagates through the Hamiltonian $H_{\Delta,l} = H_\Delta + H_l$. From the Lippman-Schwinger equation in first order approximation, we have

$$
\begin{aligned}
|\Psi_\Delta\rangle =& A \int \frac{1}{E_l} d^3p_l \frac{g_\Delta^N}{\left(E^* - H_\Delta + i\frac{\Gamma}{2}\right)} |\Delta, l\rangle_{\tau'} \\
& \times {}_{\tau'} \langle \Delta, l| g_\tau^{\tau'} |N, \nu\rangle_\tau ,
\end{aligned} \tag{10}
$$

with $E^* = E - E_l$, where E_l is the lepton energy, E is the energy of the neutrino-nucleon system and, Γ is the half-width at half maximum of the curve. In the above equation, we assume that the lepton Hamiltonian H_l corresponds to the free lepton, H_Δ is the free resonance Hamiltonian, and g_Δ^N is the resonance-nucleon coupling.

The final states are formed by a final nucleon N', a lepton and a meson. So, we project the state in the above equation on states of the form $|N', m, l\rangle$, leading

$$
\begin{aligned}
|\Psi_f\rangle =& A \int \frac{1}{E_l} d^3p_l \int d^4p_{N'} \int d^4p_m |N', m, l\rangle_{\tau''} \\
& \times {}_{\tau''} \langle N', m, l| \frac{g_\Delta^N}{\left(E^* - H_\Delta + i\frac{\Gamma}{2}\right)} |\Delta, l\rangle_{\tau'} \\
& \times {}_{\tau'} \langle \Delta, l| g_\tau^{\tau'} |N, \nu\rangle_\tau \, \delta^4(p_{N'} + p_m - p_\Delta),
\end{aligned} \tag{11}
$$

which can be integrated with respect $p_{N'}$, resulting

$$
\begin{aligned}
|\Psi_f\rangle =& A \int \frac{1}{E_l} d^3p_l \int \frac{1}{E_m} d^3p_m |N', m, l\rangle_{\tau'} \\
& \times {}_{\tau'} \langle N', m, l| \frac{g_\Delta^N}{\left(E^* - H_\Delta + i\frac{\Gamma}{2}\right)} |\Delta, l\rangle_{\tau'} \\
& \times {}_{\tau'} \langle \Delta, l| g_\tau^{\tau'} |N, \nu\rangle_\tau ,
\end{aligned} \tag{12}
$$

with $p_{N'} = p_\Delta - p_m$. Then, the transition probability reads

$$
\begin{aligned}
d\sigma_0(\tau, \tau') = |\Psi_f|^2 = A \frac{\sigma_0(\tau, \tau')}{\left[(E^* - H_\Delta)^2 + (\Gamma/2)^2\right]} d^3p_l \, d^3p_m, \\
A^{-1} = \int \frac{1}{E_l} d^3p_l \int \frac{1}{E_{N'}} d^3p_{N'},
\end{aligned} \tag{13}
$$

in the case that the final nucleon is free, where

$$
\sigma_0(\tau, \tau') = |g_\Delta^N \times \langle \Delta, l| g_\tau^{\tau'} |N, \nu\rangle|^2.
$$

When the final nucleon is bound, antisymmetrization reduces its phase-space and

$$
A^{-1} = \int \frac{1}{E_l} d^3p_l \, \Omega_{N'}, \tag{14}
$$

where $\Omega_{N'}$ corresponds to the final nucleon phase-space.

In CRISP model, $\Omega_{N'}$ is calculated by considering the Pauli blocking mechanism. So, we can normalize by setting

$$
A^{-1} = \int \frac{1}{E_l} d^3p_l. \tag{15}
$$

Finally, in this description, the only unknown quantity is $\sigma_0(\tau, \tau')$, which is independent of the particle momenta. We understood that this treatment of Δ-nucleon interaction is rough and obeys to simplicity in the present KM. A consistent formalism of the Δ-nucleon interaction from the effective Lagrangian theory was performed by Mariano *et al.* [5, 6] within the CIM.

C. On fake events

Ones of the most relevant nuclear effects are the fake events, *i.e*, states at the end of the nuclear reaction initiated by

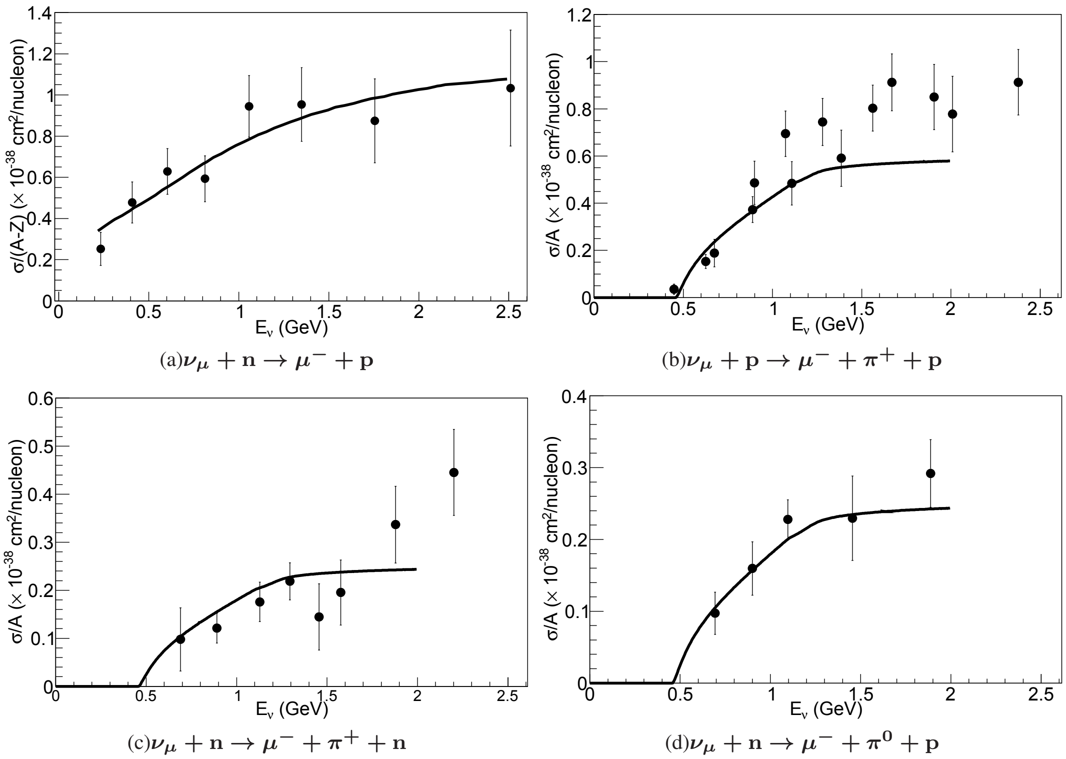

(a) $\boldsymbol{\nu_\mu + n \to \mu^- + p}$ (b) $\boldsymbol{\nu_\mu + p \to \mu^- + \pi^+ + p}$

(c) $\boldsymbol{\nu_\mu + n \to \mu^- + \pi^+ + n}$ (d) $\boldsymbol{\nu_\mu + n \to \mu^- + \pi^0 + p}$

FIG. 1. Best fitted results of KM for the ν_μ-deuterium cross section compared with experimental data from Refs. [36, 37].

the neutrino that are different from the states formed by the neutrino-nucleon primary interaction, and if they are detected could be confused with another event. This effect is a consequence of the final state interaction in the nucleus. Moreover, could to come, for instance, from the nucleon-nucleon interaction where is exchanged the energy of protons and neutrons in the binary collisions of the intranuclear cascade or, in the case where the expected nucleon in the final state remains bound to the nucleus. The output result is that the original state produced is counted in the primary interaction as a different state. We will refer to this effect as crossed channels or fake events, as they are usually called in the literature.

III. RESULTS AND ANALYSIS

A. Free parameters adjustment

In the KM the only free parameters are A_n $(n = 0, 1, 2, 3, 4)$ for the CCqe channel and $\sigma_o(\tau, \tau')$ for the CCres channel. In order to determine these parameters, neutrino-deuterium cross section on deuterium measured at Brokkhaven National Laboratory (BNL) [36] and Argone National Laboratory (ANL)[37] were used. This information is the same experimental data employed previously by O. Lalakulich and U. Mosel in their studies on pion production in the MiniBooNE experiment [16]. Here, we disregard the small nuclear effects present in the interaction with deuterium and consider the cross section as representative of the neutrino-nucleon process. In Figure 1 we present the best-fitted result for our model to the available experimental data. In Table I the corresponding values for all the parameters are displayed. One observes a nice fit of our calculation to the experimental data. In the case of the channel in Figure 1(b) (channel B of Table I) one can notice that the calculation slightly underestimates data above $E_\nu \sim 1.5$ GeV. This result can be attributed to the lack of resonances heavier than $\Delta(1232)$ in the present version of our model.

With the inclusion of the KM described in the last section into the CRISP model, we can evaluate the nuclear effects on the neutrino-nucleus interaction and calculate the inclusive neutrino-nucleus cross section up to $E_\nu \sim 1.5$ GeV.

B. Reaction cross section

The neutrino-nucleus cross sections are determined employing the CRISP code by calculating the frequency of appearance of a previously obtained channel from a number N_0 of total events. So then, the cross section reads

$$\sigma_{ev} = \sigma_g \frac{N_{ev}}{N_0}, \tag{16}$$

where N_{ev} is the number of events that ended within the concrete channel under analysis, and $\sigma_g = \pi r_0^2 A^{2/3}$, is the nucleus geometric cross section, with A being the mass number and $r_0 = 1.2$ fm.

We consider as an event, to anything of the final configuration listed in Table I. The calculations are performed for the two kinds of events, namely true-type and like-type events. A true-type event is when the final configuration is exactly as those listed above, while a like-type event is when the configuration exists amid other particles.

The total cross sections for each channel are shown in Figure 2 for all nuclei studied in the present work.

In Figure 3 the calculated CCqe cross section are compared with the available experimental data on ^{12}C. We observe an overall agreement between calculation and experimental data in the like-type events, while on the true-type events the theoretical calculations underestimate the data. The diminishing in the nuclear cross section in the last case is mainly attributable to events where the proton in the final state remains bond in the nucleus.

In the CRISP model, the nucleus is described as a Fermi gas in a square-well potential, which is a fair description for heavier nuclei, but is not adequate for ^{12}C. Unfortunately, there are not any experimental data for other nuclei or channels, but one can expect that this nuclear structure effect is less important for heavier nuclei.

One can notice in Figure 2 that there is an overall decreasing in the cross sections when the nuclear mass increases. Although the nuclear level structure here considered, corresponding to a square-well potential, it has some noticeable effects on the relative cross sections. To better visualizes this effect, in Figure 4 we present the calculated cross section (σ_X) normalized to the ^{12}C cross section (σ_{12C}) for six different nuclei: $X = \{^{16}\mathrm{O}, ^{27}\mathrm{Al}, ^{40}\mathrm{Ar}, ^{56}\mathrm{Fe}, ^{208}\mathrm{Pb}\}$, for both true-type and like-type events. Two general aspects are observed: (i) there is a fast increase in $\mathcal{R} = \sigma_X/\sigma_{12C}$ for all nuclei at low neutrino energy and, (ii) there is an explicit dependence on the nuclear mass.

The diminishing in the cross section is due to nuclear effects, since it depends on the nuclear mass. In fact, as the nucleon produced in the final state after the neutrino-nucleon interaction propagates inside the nuclear matter, it can transfer its energy to other nucleons, so in many cases, the particles emitted from the nucleus are not exactly those formed in the neutrino-nucleon interaction.

Since the average length of the distance traveled by a nucleon increases with the nuclear mass, also the probability of crossed channels increases. This effect reduces, therefore, the observed cross section, as can be noticed in Figure 4.

The rise in the ratio of low energies, $\mathcal{R}$, is related to the escape of the nucleon produced in the primary interaction of the nucleus. At low energy, most of the neutrino energy goes to the muon production, leaving the nucleon with low energy, so it can not overcome the nuclear barrier. The result is that one has a crossed channel event. Over of the region of fast increase of $\mathcal{R}$, appears a plateau that it remains approximately constant for all nuclei and channels. In this region, the produced nucleon has enough energy to escape from the nucleus. However, in its way out the nucleon will interact with others nucleons and eventually, a charge-exchange collision will produce a crossed channel. Then, as larger is the nucleus as higher is the probability of crossed channel events, and for the CCqe case, we have checked that this probability is roughly proportional to $A^{1/3}$.

The same reasoning applies qualitatively to the resonant channel. However, in these cases, the reaction mechanism is more complicated because the resonance propagates inside the nucleus exchanging energy with other nucleons, which will produce other effects that superpose to the ones described above. For example in Ref. [38], the authors have presented detailed calculations performed in ^{12}C showing that the two-particle two-hole is the mainly contribution of multinucleon excitations. Many of these effects are related by the influence of short range correlations (SRCs) on the one-nucleon (1N) and two-nucleon (2N) knockout channels, and to two-body currents arising from meson-exchange currents. For the channel of the like-type, the results for $\mathcal{R}$ are very similar to the true-type.

Another real nuclear effect on the neutrino-nucleus interaction can be observed in the calculated cross sections for nuclei, as shown in Figure 3 , as compared to the interaction on nucleon, as shown in Figure 2. In fact, one can observe that the interaction threshold is around 0.45 GeV in the nucleon case, while the threshold is below that energy for nuclear interactions. This subthreshold interaction is due to the Fermi motion of bound nucleons, and it is a natural consequence of our calculations using the CRISP model. In fact, these kinds of phenomena can also be observed for other processes [21]. Goldhaber and Shrock [22] relating by first time the possible subthreshold reactions involving nuclear fission such as: (i) photo-fission with pion-production and, (ii) charged-current neutrino-nucleus reactions that lead to fission and/or to the formation of a Coulomb bound state of a μ^- with the nucleus of a fission fragment, that is a very similar to the reactions studied in this work.

In Figure 4 we analyze the like-type events as compared to the true-type ones. The like-type cross sections are always higher since these counts the true-type events and also more complex configurations. With the CRISP model, it is possible to disentangle the various contribution to the like-type cross section, as shown in the Figure 5 for some of the more simple configurations. In such figure, we showed the partial contributions from some final state configuration to the like-type cross section for ^{56}Fe and ^{12}C in the CCqe channel and the CCres channel like-type. The addition of like-type, 1p+1n, 2p+1n, 1p+2n, 2p+2n in (dashed lines), and the true-type in (solid line) are also shown for comparison. In both nuclei in consideration, the sequence of contributions is similar: main contribution from 1p+1n, in second place 2p+1n plus 1p+2n, and finally the 2p+2n, more closed to the true-type in the last reactions. For the CCqe reactions the true-type and like-type are broadening in ~ 0.3 GeV, whereas for CCres this "threshold" is in ~ 0.4 GeV due the nuclear delta liberty grade.

As one allows more and more complex configurations, the cross section rises from the true-type cross section to the like-type cross section, where are considered all possible configurations. It is also possible to observe that increasing the neutrino energy, the complexity of like-type events increases, while at low energy true-type and like-type almost coincides. Comparing the CCqe and the resonant channels, we note that the several trends and relative contribution of a different channel are similar.

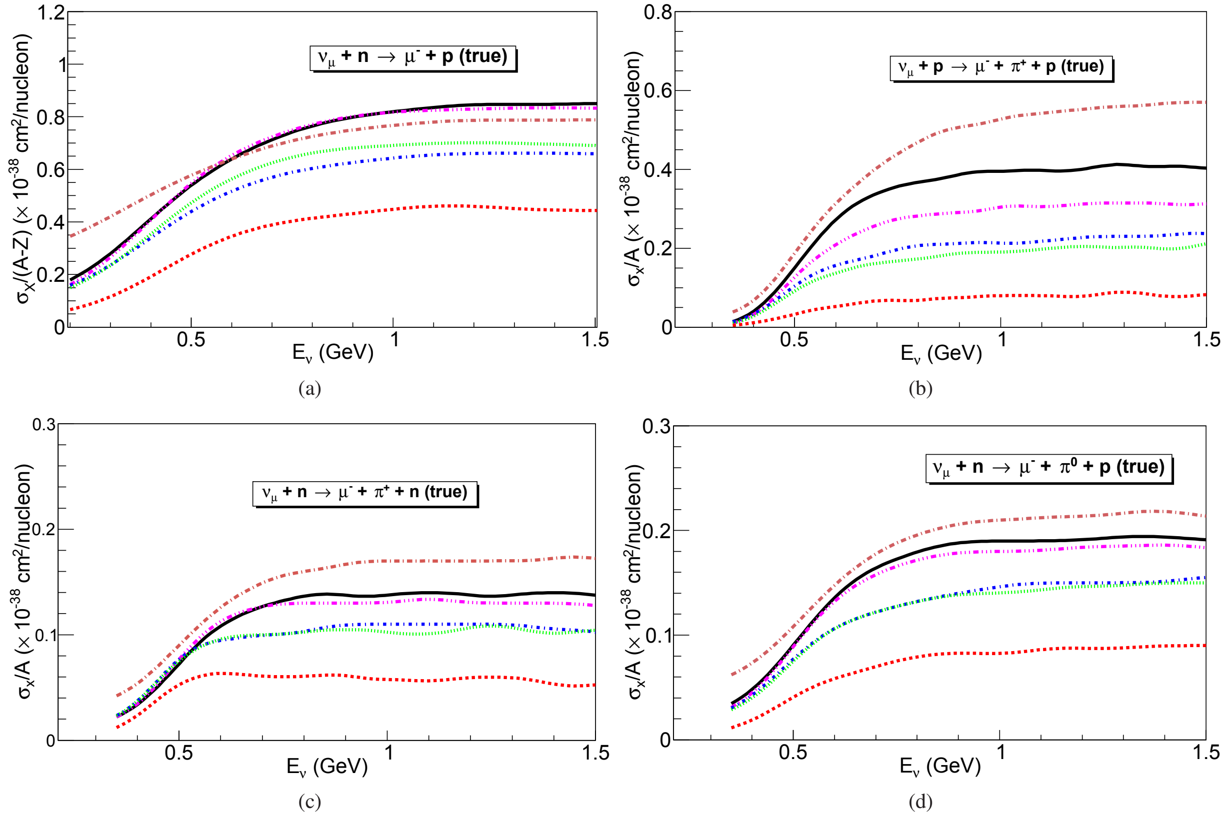

FIG. 2. (Color online) ν_μ-A cross sections for all true-type channels studied as function of neutrino energy for all nuclei: (long dash dot brown line) ^{12}C, (solid black line)^{16}O, (dash dot rouge line) ^{27}Al, (dash dot blue line) ^{40}Ar, (dot green line) ^{56}Fe, and (dot red line) ^{208}Pb.

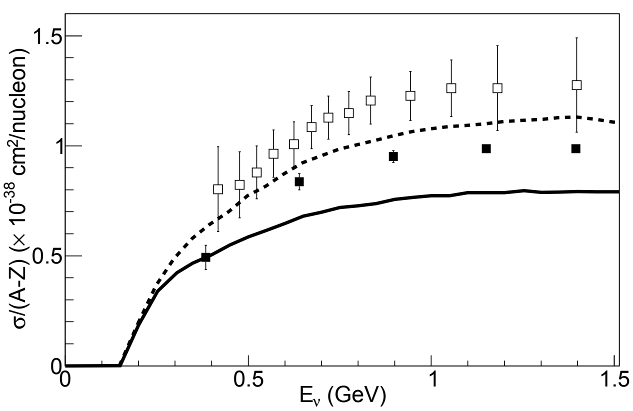

FIG. 3. ν_μ-^{12}C cross section within KM model according true-type (solid line) and like-type (dashed line) events for $\boldsymbol{\nu_\mu + \mathrm{n} \rightarrow \mu^- + \mathrm{p}}$ channel. The experimental data for true-type (filled squares) [9] , and like-type (hole squares) [11] are shown for comparison.

In general, one can see that real nuclear effects are of great importance to understand the neutrino-nucleus interaction. These results are relevant since some cross section (^{208}Pb for instance) can be reduced to about 20% of the ^{12}C one due to these effects.

The interaction with the nucleus of the particles produced in the primary interaction is responsible for the more intense effects, reducing the cross section per nucleon as the nuclear mass increases. At low energy, however, the binding energy is more important, and probably nuclear structure will be necessary to completely understand the process for neutrino energy up to ~ 0.5 GeV. In this direction, a recent work within the Continuum Random Phase Approximation (CRPA) has calculated the $(\nu_\mu/\bar{\nu}_\mu)-^{12}$C cross section in kinematics conditions for MiniBooNE and T2K. The cross sections have shown to be comparable with the experimental data, but underestimating the MiniBooNE data for backward muon scattering angles, where the missing strength can be associated with the contribution from multinucleon knockout and single-pion production processes. Among other microscopical models that can be useful in this region is the Relativistic Quasiparticle RPA [39], that studied the evolution of the configuration space number below 0.3 GeV. In this energy interval, the cross sections converge for sufficiently large configuration space and final-state spin and could be joined smoothly with the Relativistic Fermi Gas including at least $1N$ and $2N$ knockout reaction in the same way as in Ref. [38].

C. Analysis of fake events/crossed channels

With the CRISP model used in the present analysis, it is possible to evaluate the amount of crossed channels in the

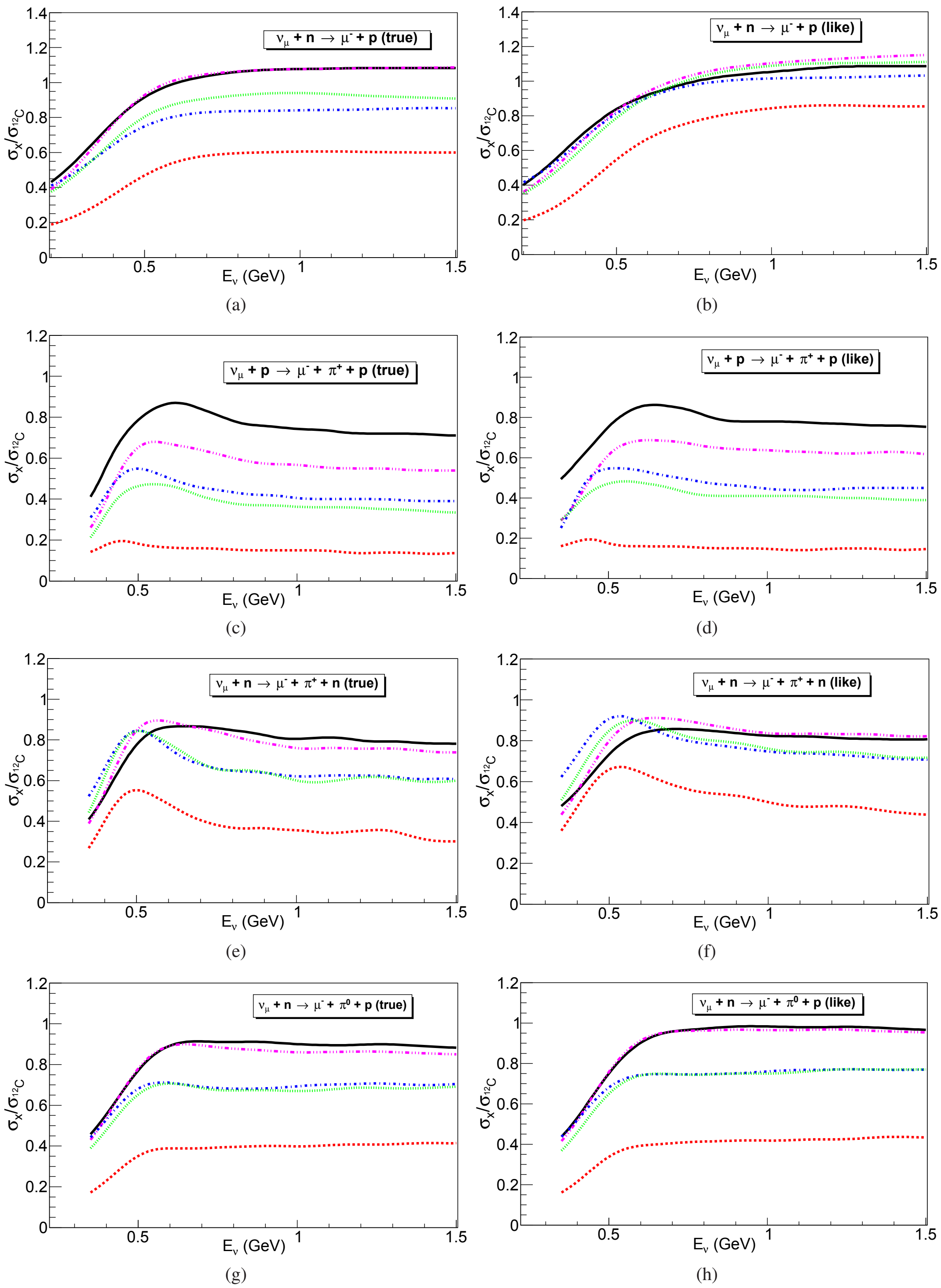

FIG. 4. (Color online) Inclusive muon neutrino-nucleus cross section ratios relative to ^{12}C, $\mathcal{R} = \sigma_X/\sigma_{12C}$, for different channels as function of neutrino energy: (solid black line)^{16}O, (dash dot dot dot rouge line) ^{27}Al, (dot green line) ^{56}Fe, (dash dot blue line) ^{40}Ar, (dot red line) ^{208}Pb. Left panel: true-type and Right panel: like-type events.

neutrino-nucleus interaction. This process is done by counting the number of primary events in the channel "i", $N_p(i)$, and the number of those events that remains in the channel after the intranuclear cascade is completed, $N_f(i)$. The number of crossed channels events is given by

$$N_c(i) = N_p(i) - N_f(i), \tag{17}$$

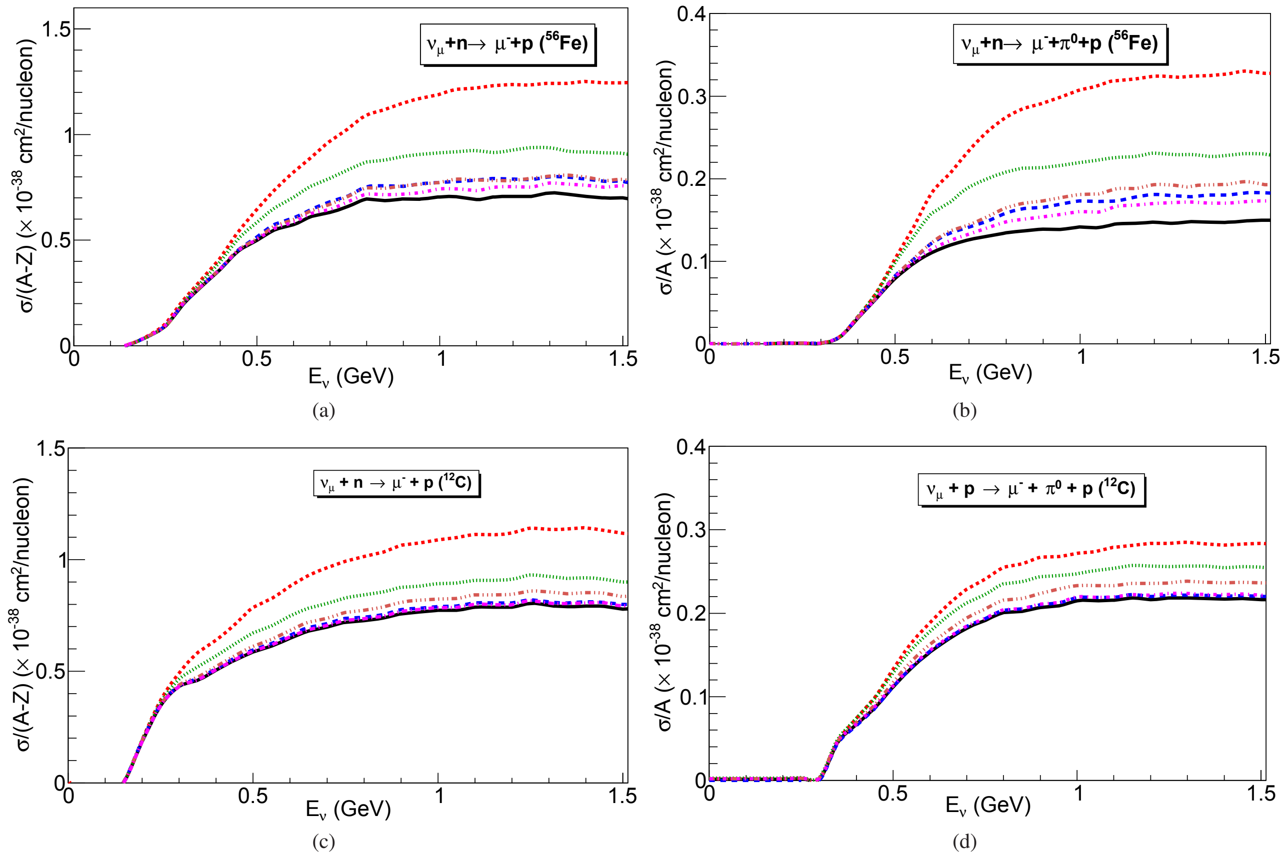

FIG. 5. (Color online) Partial contributions from some final state configuration to the like-type cross section for ^{56}Fe and ^{12}C in the CCqe channel (left panel) and the CCres channel (right panel). We show the contributions: added like-type (dash red line), 1p+1n (dot green line), 2p+1n (dash dot brown line), 1p+2n (long dash blue line), 2p+2n (dash dot pink line), and finally the true-type (solid black line).

also, the fraction of crossed channels events is

$$R_c(i) = \frac{N_c(i)}{N_p(i)}. \tag{18}$$

In Figure 6 are shown the percentage of false events, $R_c(i)$ according to Eq. (18), as a function of neutrino energy for CCqe channels for the studied target nuclei: ^{12}C, ^{16}O, ^{27}Al, ^{40}Ar, ^{56}Fe and ^{208}Pb. We note that the ratio is initializing in 250 MeV with the higher value ($\approx 80\%$) and then it goes to an averaged constant value. The behavior is similar to all the target nuclei except for ^{12}C, mainly due that the Fermi gas model is not a good description for light nuclei as carbon. We can intuit that the saturation effect of $R_c(i)$ is because the neutrino has reached the maximum of interactions within the space of possible configurations of type $xp - xn$ created inside the nucleus over 0.5 GeV. This fact must be revised when we will include in our simulation more channels coming from resonances higher than $\Delta(1232)$.

In Table II we present the results of fake events obtained with CRISP using KM and CIM formalism for the CCqe and CCres channels in ^{12}C, ^{16}O, ^{27}Al, ^{40}Ar, ^{56}Fe and ^{208}Pb. The CIM model cross sections as a function of the neutrino energy [5] were fitted to a fourth degree polynomial to include in CRISP. In the first column of Table II, we shown the

TABLE II. Percentage (%) of fake events, $R_c(i)$ according to Eq. (18), when one uses the KM and CIM methodologies [5, 6].

Channel	^{12}C	^{16}O	^{27}Al	^{40}Ar	^{56}Fe	^{208}Pb
A-KM	30	34	40	50	50	64
A-CIM	30	34	38	48	48	66
B-KM	50	58	68	76	82	90
B-CIM	48	60	70	78	80	90
C-KM	82	86	88	92	94	98
C-CIM	84	88	90	92	94	96
D-KM	62	70	74	78	80	88
D-CIM	64	70	74	80	82	88

channels interaction labeled as in Table I. The next columns shown the evolution of percentage of fake events as increasing mass number according to the target nuclei. The table can go through a solid nucleus mass analyzing the contribution for each channel. The inputs of the A channel are lower for all the nuclei, following in ascending order D and B. The maximum is obtained from C reaction ($\nu_\mu + n \to \mu^- + \Delta^+ \to \mu^- + \pi^+ + n$) for all the target nuclei being in average ≈ 90 %. On the other point of view, relative to the channel reaction, we note that the fake events increase as well the mass increases,

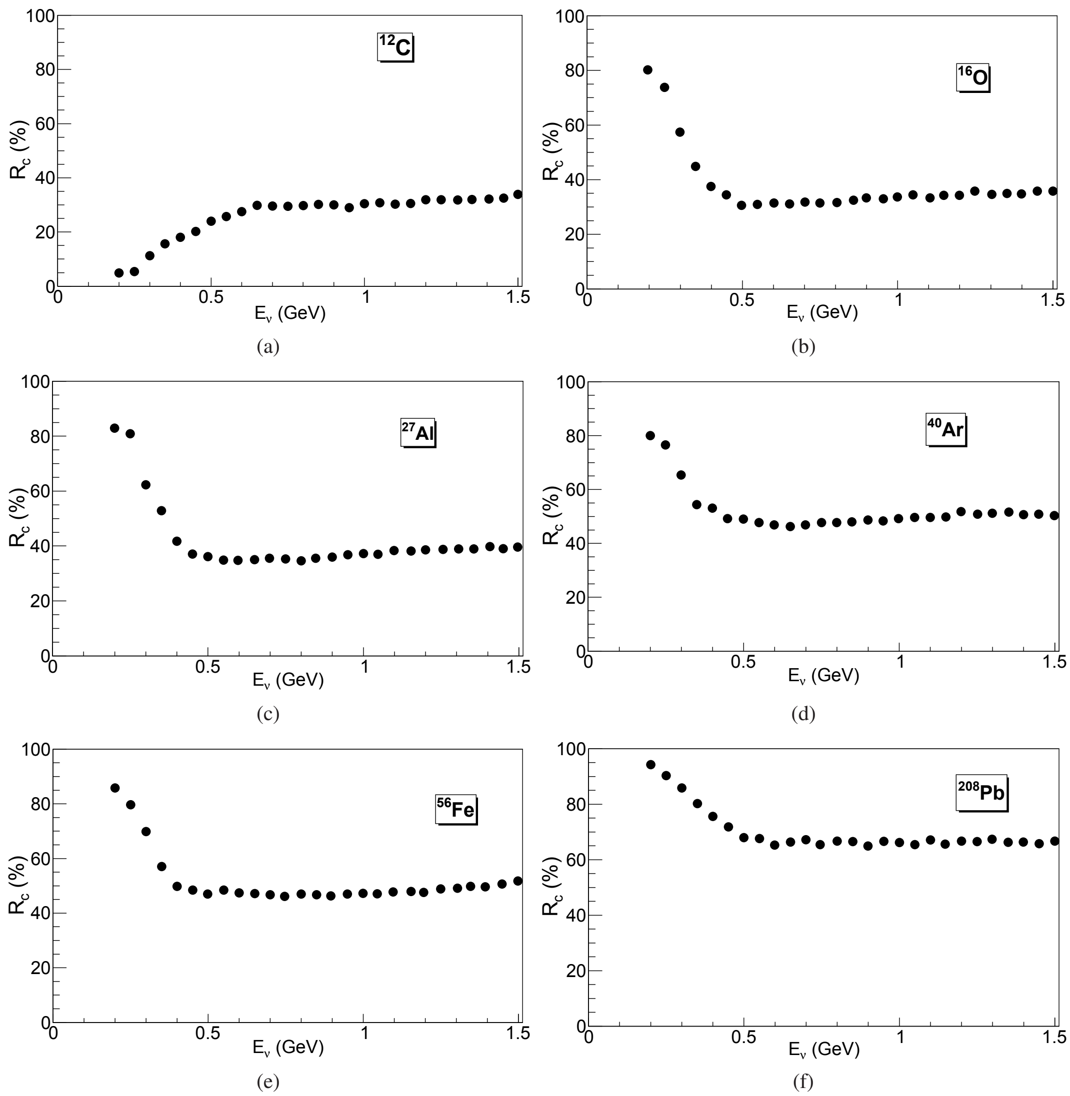

FIG. 6. Percentage of false events, $R_c(i)$ according to Eq. (18), as function of neutrino energy for CCqe channels for the studied target nuclei: a) ^{12}C, b) ^{16}O, c) ^{27}Al, d) ^{40}Ar, e) ^{56}Fe and f) ^{208}Pb.

being minimal in carbon and maximum in the lead. Summarizing, we can observe that with the growth in the atomic number and atomic mass of the target nucleus, which increases the percentage of false events due to the appearance of the nuclear structure effects and the interactions among the several nucleons.

The employment of different formalisms like KM and CIM for the neutrino cross section of primary interaction has almost any effect on the percentage of false events because they are a direct consequence of the intranuclear cascade and not of primary exchanges.

D. Energy distribution of the emitted pions and muons

The pion spectrum in the CRISP model is calculated as

$$\frac{d\sigma}{dT_\pi} = \sigma_g \frac{N_{ev}(T_\pi)}{N_0 \Delta T_\pi},$$

awhere $N_{ev}(T_\pi)$ is the number of events for a specific channel producing a pion with a given isospin with energy between T_π and $T_\pi + \Delta E_\pi$. The MiniBooNE experiment measured the positive pion spectrum for $E_\nu \sim 1$ GeV on ^{12}C [10, 11]. In the left panel of Figure 7, we show our calculation averaged over the published MiniBooNE flux for π^+ [12] in comparison with the experimental data. We observe that both calculation and data show a similar shape with the peak around 80 MeV and a large tail at high energies. Quantitatively there is a good agreement between calculation and experiment, notably in the peak region. At energies above 250 MeV, the calcu-

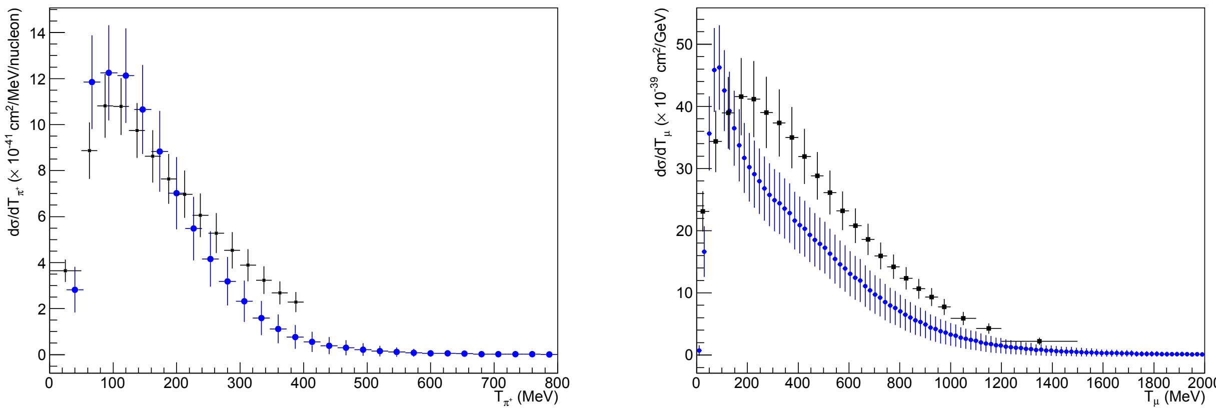

(a) (b)

FIG. 7. Energy distribution for π^+ (left panel) and μ^- (right panel), for reaction induced with ν_μ with the energy of $\sim$ 1 GeV on ^{12}C. Experimental data (black cross) of MiniBooNE [10, 11] are also shown for comparison. The error bars in the theoretical calculations are statistical due the propagation of error in the Monte Carlo and from the deviation in the neutrino flux.

lation underestimates the experimental data. It is likely that this effect is related to that we were not included higher mass resonances in the present calculations.

Similarly, the ejected muon distribution is calculated as a function of the kinetic muon energy as

$$\frac{d\sigma}{dT_\mu} = \sigma_g \frac{N_{ev}(T_\mu)}{N_0 \Delta T_\mu}.$$

The right panel of Figure 7 shows the muon distribution calculation as a function of the kinetic muon energy, averaged over the published MiniBonNE flux for π^+ [12], in comparison with the experimental MiniBooNE data for $E_\nu \sim 1$ GeV. Here, we note that our theoretical calculation is slightly lower than the experimental results, but the behavior and the peak position are in a well agreement with data. Relative to these calculations: (i) we do not adjust the pion mass resonances to reproduce the experimental spectra as it was done by Lalakulich and Mosel *et al.* in [16]; (ii) we are taken into account only the contribution of the delta resonance, for this reason, we do not implement other reaction channels in the neutrino generator with other resonances, presented in the intranuclear cascade in these calculations and; (iii) our formalism is not including an angular distribution for the ejected particle. Then, our model will not be in completely agreement with some experimental data, in comparison with another model performed by such issue. Also, it is important to remember that we use a Fermi gas model, which is not the best choice, especially for ^{12}C, so that structure does not have any physical significance.

Some final words are devoted to the comparison with another theoretical model, as such that performed in Ref. [16]. The analysis performed here is in many aspects similar to the one presented in Ref. [16], where medium's effects on neutrino nucleus interaction were studied. The most relevant differences between the approach used here and that in Ref. [16] are related to the modeling of the bound nucleon dynamics. A summary of these differences is the following:

1. In the CRISP model the nucleus is described as a global Fermi gas, while in Ref. [16] is used a local Thomas-Fermi approach.

2. As a consequence of the first difference, in CRISP model the Pauli blocking mechanism is accounted for strictly, while in Ref. [16] it is considered statistically. Careful analysis of the advantages of a strict Pauli blocking mechanism are presented in Refs. [17, 35].

3. With the inclusion of Fermi motion and rigorous Pauli blocking, some nuclear effects emerge naturally in the calculations with the CRISP model, such as shadowing effect, that is present in photoabsorption and in meson production, for example in Refs. [26, 40]. Also, medium's effects on resonance propagation are naturally accounted in the CRISP model.

These differences are relatively more important for energies near the reaction threshold, and should practically disappear as the incoming particle energy increases. At first sight, the aspects mentioned above could explain why the CRISP model gives better results as compared to experimental data than the calculations in Ref. [16], however the disagreement between the both calculations seems to be too large to be attributed only to those different methods used in each model.

The medium's modifications in Δ resonance, for instance, were first observed in photoabsorption measurements and were mainly attributed to Fermi motion and Pauli blocking effects [41–43], although some effects from the coherent sum of resonant and direct channels could be observed [44]. In Ref. [16] the authors inform to have included the Δ resonance broadening through the Salcedo and Oset model [45], but in their spectral function are also encompassed for the bound nucleon, both Fermi motion and Pauli blocking effects. It is possible, then, that the Δ resonance broadening is taken into account twice: one time in the modeling of the resonance, and the another time by the nuclear effects already considered in their nuclear model. This way of counting could explain why their calculation underestimates the cross section in the resonance peak energy, since the broadening of the resonance width results in a reduction of the cross section at the peak. Also, it can explain the shift of the peak energy to lower energies, since the combination of Fermi motion and Pauli blocking produces such effect.

IV. CONCLUSION

In the present work we report an extensive analysis of nuclear effects in neutrino-nucleus interaction. For this purpose, a simple model of neutrino-nucleon, which was called Kinetic Model, is used together with the CRISP model to take into account the nuclear effects. This simple model has three free parameters for all channels analyzed in this study. We determined these parameters by fittings to the specific channels to neutrino-deuterium experimental data.

The calculations were performed for neutrino energies from 0.2 to 1.5 GeV for ^{12}C, ^{16}O, ^{27}Al, ^{40}Ar, ^{56}Fe and ^{208}Pb. We calculated the cross section for all nuclei in the whole energy range using CCqe and CCres channels. Where data is available, a comparison between calculation and experiment was provided. The pion and muon spectra are also calculated and compared to the experimental data showing a fair agreement.

For the set of target nuclei employed, we performed an exploratory study of the fake events generated in several reactions. This study has shown that the percentage of CCqe fake events for ^{12}C, important for MiniBooNE, are in the same order of ≈ 30 % of previous works [14, 16]. Whereas than for other nuclei the percentage of fake events increases as well the nuclei masses increases due to the structure effect and multinucleon excitations in the nucleus. Using two different formalisms of neutrino-nucleon cross sections was shown than the percentage of fake events are almost independent of the primary interactions because they are a direct consequence of intranuclear cascade. In a future work, we will improve the simple Kinetical Model used for the primary interaction using the Consistent Isobar Model-CIM [5, 6].

Our conclusions are that nuclear effects are decisive for understanding the neutrino-nucleus interaction, and the most substantial effect is the interaction of the produced particles with the nucleus. Another important effect that appears mainly for neutrino energies below ~ 0.5 GeV are the nuclear binding energy, Fermi motion and Pauli blocking. For all studied channels, we observed the subthreshold reaction. Finally, we predict that nuclear structure plays a relevant role in this energy range.

ACKNOWLEDGMENTS

Part of this work was performed in the frame of the academic cooperation agreement between UESC and InSTEC. O. Rodríguez and F. Guzmán would like to recognize the provisions of UESC for the conclusion of this work. D. Vargas, A. R. Samana and F. Velasco thank the financial support of Fundação de Amparo à Pesquisa do Estado da Bahia (FAPESB) and CAPES-AUXPE-FAPESB-3336/2014/Processo no: 23038.007210/2014-19. A. Deppman thanks the financial support of CNPq/305639/2010-2. C.Barbero and A. Mariano are fellows of the CONICET, CCT La Plata (Argentina) and thank for partial support under Grant PIP No 0349. We sincerely thank Professor Juan J. Godina-Nava for his very careful and judicious reading of the manuscript.

Finally, the authors thank the financial support of Brazilian agencies CNPq and CAPES.

[1] K. Gallmeister, U. Mosel, and J. Weil, Phys. Rev. C **94**, 035502 (2016).
[2] K. Langanke and G. Martínez-Pinedo, Journal of Physics G: Nuclear and Particle Physics **703**, 012008 (2016).
[3] C. Andreopoulos *et al.*, The GENIE neutrino Monte Carlo generator, available in: http://www.genie-mc.org, (2009).
[4] D. Casper, Nuc. Phys. B (Proc. Suppl.) **112**, 161 (2002).
[5] C. Barbero, G. López Castro, and A. Mariano, Phys. Lett. B **664**, 70 (2008).
[6] A. Mariano, C. Barbero, and G. López Castro, Nucl. Phys. **A849**, 218 (2011).
[7] M. H. Ahn *et al.*, Phys. Rev. D **74**, 072003 (2006).
[8] A. Rodríguez *et al.*, Phys. Rev. D **78**, 032003 (2008).
[9] B. Eberly *et al.* (on behalf of MINERvA collaboration), Phys. Rev. D **92**, 092008 (2015).
[10] A. Aguilar-Arevalo *et al.*, Phys. Rev. D **81**, 092005 (2010).
[11] A. Aguilar-Arevalo *et al.*, Phys. Rev. D **83**, 052009 (2011).
[12] A. Aguilar-Arevalo *et al.*, Phys. Rev. D **79**, 072002 (2009).
[13] C. Wilkinson, *et al.*, Phys. Rev. D **93**, 072010 (2016).
[14] M.Ericson,M.V. Garzelli, C. Giunti, M. Martini, Phys. Rev. D **93**, 073008 (2016).
[15] T. Leitner and U. Mosel, Neutrino interactions with nucleons and nuclei, INT Seattle WU, http://www.int.washington.edu/talks/WorkShops/int_10_2b/People/Mosel_U/Mosel.pdf (2010).
[16] O. Lalakulich and U. Mosel, Phys. Rev. C **87**, 014602 (2013).
[17] A. Deppman, S. B. Duarte, G. Silva, O. A. P. Tavares, S. Anéfalos, J. D. T. Arruda-Neto, and T. E. Rodrigues, Journal of Physics G: Nuclear and Particle Physics **30**, 1991 (2004).
[18] M. Gonçalves, S. de Pina, D. Lima, W. Milomen, E. Medeiros, and S. Duarte, Phys. Lett. B **406**, 1 (1997).
[19] A. Deppman, O. A. P. Tavares, S. B. Duarte, E. C. de Oliveira, J. D. T. Arruda-Neto, S. R. de Pina, V. P. Likhachev, O. Rodriguez, J. Mesa, and M. Gonçalves, Phys. Rev. Lett. **87**, 182701 (2001).
[20] E. Andrade-II, J. C. M. Menezes, S. B. Duarte, F. Garcia, P. C. R. Rossi, O. A. P. Tavares, and A. Deppman, Journal of Physics G: Nuclear and Particle Physics **38**, 085104 (2011).
[21] I. González, F. Guzmán, and A. Deppman, Phys. Rev. C **89**, 054613 (2014).
[22] M. Goldhaber and R. Shrock, Phys. Rev. C **63**, 021303 (R)

(2001).
[23] E. Andrade-II, I. González, A. Deppman, and C. A. Bertulani, Phys. Rev. C **92**, 064903 (2015).
[24] V.P. Likhachev, *et al.*, Phys. Rev. C **68**, 014615 (2003).
[25] I. Gonzalez, C. Barbero, A. Deppman, S. Duarte, F. Krmpotić, and O. Rodriguez, Journal of Physics G: Nuclear and Particle Physics **38**, 115105 (2011).
[26] I. Gonzalez, A. Deppman, S. Duarte, F. Krmpotić, M. S. Hussein, and C. Barbero, Journal of Physics: Conference Series **312**, 022017 (2011).
[27] T. Kodama, S. B. Duarte, K. C. Chung, and R. A. M. S. Nazareth, Phys. Rev. Lett. **49**, 536 (1982).
[28] A. Deppman *et al.*, Computer Physics Communications **145**, 385 (2002).
[29] A. Deppman *et al.*, Nuclear Instruments and Methods in Physics Research Section **B**: Beam Interactions with Materials and Atoms **211**,15 (2003).
[30] A. Deppman, G.S. Karapetyan, V. Guimaraes,C. Gonzales, A.R. Balabekyan,N.A. Demekhina, Phys. Rev. C **91**, 024620 (2015).
[31] F. G. Velasco, F. Guzmán, O. Rodriguez, O. Tumbarell, D. A. Souza, A. R. Samana, E. Andrade-II, J. L. Bernal Castillo, and A. Deppman, Brazilian Journal of Physics **46**, 415 (2016).
[32] U. Brosa, S. Grossmann, and A. Müller, Phys. Rep. **197**, 167 (1990).
[33] A. Deppman, E. Andrade-II, V. Guimarães, G. S. Karapetyan, A. R. Balabekyan, and N. A. Demekhina, Phys. Rev. C **88**, 024608 (2013).
[34] A. Deppman, E. Andrade-II, V. Guimarães, G. S. Karapetyan, O. A. P. Tavares, A. R. Balabekyan, N. A. Demekhina, J. Adam, F. Garcia, and K. Katovsky, Phys. Rev. C **88**, 064609 (2013).
[35] T. E. Rodrigues, J. D. T. Arruda-Neto, A. Deppman, V. P. Likhachev, J. Mesa, C. Garcia, K. Shtejer, G. Silva, S. B. Duarte, and O. A. P. Tavares, Phys. Rev. C **69**, 064611 (2004).
[36] T. Kitagaki, *et al.*, Phys. Rev. D **34**, 2554 (1986).
[37] S.J. Barish, *et al.*, Phys. Rev. D **19**, 2521 (1979).
[38] T. VanCuyck, N. Jachowicz, R. Gonzalez-Jimenez, M. Martini, V. Pandey, J. Ryckebusch, N. VanDessel, Phys. Rev. C **94**, 024611 (2016).
[39] A. R. Samana, F. Krmpotić, N. Paar and C. A. Bertulani, Phys. Rev. C **83**, 024303 (2011).
[40] A. Deppman, G. Silva, S. Anefalos *et al.*, Phys. Rev. C**73**,064607 (2006).
[41] N. Bianchi, V. Muccifora, A. Deppman *et al.*, Phys. Lett. **B309**, 5 (1993).
[42] N. Bianchi, A. Deppman, E. Desanctis *et al.*, Phys. Lett. **B299**, 219 (1993).
[43] M. Mirazita, H. Avakian, N. Bianchi *et al.*, Phys. Lett. **B407**, 225 (1997).
[44] K. Ochi, M. Hirata, T. Takaki Phys. Rev. C **56**, 1472 (1997).
[45] E. Oset and L. Salcedo, Nucl. Phys. **A468**, 638 (1987).